*32nd URSI GASS, Montreal, 19–26 August 2017*

# Electromagnetic Pulse Emissions from Hypervelocity Impacts on Charged Targets

Andrew Nuttall*(1), Ashish Goel(1), Sigrid Close(1), and Ivan Linscott(1)
(1) Stanford University

## Abstract

Hypervelocity impacts with dust-sized meteoroids and space debris are a routine occurrence for spacecraft. While the potential for mechanical damage from sub-nanogram mass impactors is negligible, unwanted electrical effects can occur via the impact plasma cloud. This paper investigates into the potential production of strong electromagnetic pulses (EMPs) created by hypervelocity impacts on charged spacecraft surfaces. Experiments were conducted at ground-based facilities to recreate impacts under different spacecraft charging conditions. The effects of impactor mass, velocity, and spacecraft charge state on electromagnetic pulse production were investigated. Novel signal processing techniques were developed to isolate the radio-frequency (RF) emissions associated with impact, and plasma theory derived time dilations were developed to allow for impact data aggregation. Our data shows wideband RF pulses were detected within 450 ns after impact on targets with a strong negative bias. Scaling laws were developed to determine the dependence of EMP peak electric field strength with impactor mass and velocity. The derived scaling indicates that impacts on strongly negatively biased spacecraft can produce peak electric fields in excess of $10^4$ V/m, placing spacecraft electronics at risk.

## 1 Introduction

Spacecraft are routinely impacted by space debris and meteoroids [1, 2]. The velocity regime ($> 7$ km/s), in which these impacts occur classifies them as hypervelocity impacts, which expose a spacecraft to both mechanical and electrical effects. An impact is classified as hypervelocity when it occurs at speeds faster than the local speed of sound of the impacted material. During hypervelocity impacts, shock waves are generated in both the target and impactor, and the rapid deposition of heat into the material leads to vaporization and ionization of both the impactor and a portion of the spacecraft [3]. The plasma produced from this impact is the conduit for many of the electrical effects associated with impact [6, 7, 8]. This paper focuses on the detection, characterization, and scaling of electromagnetic pulses (EMPs) in the radio-frequency (RF) spectrum induced by impacts on charged spacecraft surfaces.

The postulated EMP emission mechanism examined in this paper is through the bulk acceleration of electrons in the impact plasma by external electric fields created by charged spacecraft surfaces. For impacts that occur on a strongly biased target, we postulate that a bulk charge separation and acceleration occurs in the impact plasma when the plasma's Debye length approaches its spatial length. This bulk charge acceleration creates a wideband RF pulse that could potentially damage or interfere with sensitive electronic components.

To investigate into the emission of EMPs from impacts on charged spacecraft surfaces, experiments were conducted at multiple electrostatic accelerator facilities. Through these experiments, we confirmed and characterized the existence of an EMP associated with impact, proposed the mechanism behind its emission, and developed an understanding of how the strength of the EMP scales with impactor mass and velocity.

## 2 Experiments

To investigate the hypervelocity impact phenomena, ground-based experiments were performed at electrostatic accelerator facilities. Three experimental campaigns were undertaken, two at the Max Planck Institute (MPI) [7, 8], and one at the Colorado Center for Lunar Dust and Atmospheric Studies (CCLDAS) . These experiments were designed to recreate the high vacuum, high impact velocity conditions that can occur between orbital debris and meteoroids and spacecraft. Iron particles were impacted into targets under different charging conditions in an attempt to detect and characterize the production of EMPs from impact. To observe the impact phenomena, simultaneous optical, plasma, and RF measurements are taken during the microseconds surrounding impact. The sensor suite used at the CCLDAS facility can be seen in Figure 1.

## 3 Data Analysis

A significant challenge in detecting and characterizing EMPs from impact is posed by the low impactor masses that electrostatic accelerator facilities use. The experiments collected data from impactors with masses ranging from $10^{-16}$ to $10^{-19}$ kg. These small impactors produce very little impact plasma, and as such produce very weak EMPs when compared to some of the larger impactor masses that can be naturally found in Earth's orbit. To aid in EMP detection

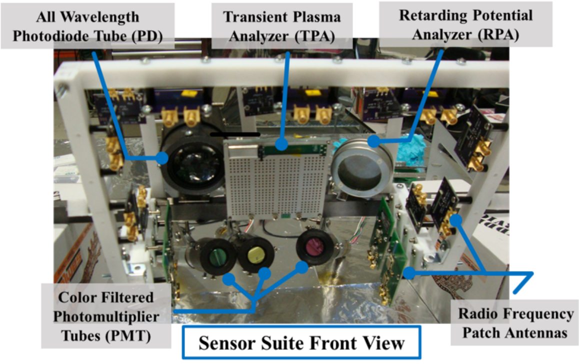

**Figure 1.** The sensor suite used at CCLDAS contained RF, optical, and plasma sensors position 10–20 cm from the impact site. An array of 165 MHz patch antennas was used in addition to stand alone 315 MHz and 916 MHz patch antennas. A similar sensor suite was used at MPI.

and isolation, a noise filtering technique called prior constrained source separation (PCSS) was developed [4]. To further promote the impact EMPs above the noise floor and to create a statistically significant database to draw conclusions from a time dilation technique was developed to allow easy aggregation of RF data across multiple impact events. The following subsections detail the noise filter, time dilation, and detection and aggregation techniques that were applied to the impact RF observations.

### 3.1 Noise Filtering

To isolate RF emissions from impact, a novel signal processing technique called prior constrained source separation was developed. PCSS uses prior knowledge to estimate and extract identified sources of noise from a measurement. The RF spectrum is dominated by cell phones, wi-fi, broadcast stations, and other consumer electronic sources. While the content of these signals is unknown, they have known parameters such as frequency allocation and modulation schemes that can be leveraged in their estimation in the form of constraints [4].

A solution for the sources of noise to be modeled **S**, and their relatives gains **A**, is estimated by maximizing the posterior probability of the model (**S**, **A**), constrained by the available prior information about each signal:

$$\underset{\mathbf{A},\mathbf{S}}{\operatorname{argmax}}\ F_{Obj}(\mathbf{A},\mathbf{S}) := \{P(\mathbf{A},\mathbf{S} \mid \mathbf{x}) \,|\, \mathbf{A} \in S_A, \mathbf{S} \in S_S\} \quad (1)$$

In this formulation $P(\mathbf{A},\mathbf{S} \mid \mathbf{x})$ is the probability of the model given the observation, $S_A$ is the set of feasible mixing matrices, and $S_S$ is the set of feasible source signals constrained by prior information. An example of this noise filtering technique is shown in Figure 2, where sources of noise were modeled and extracted to better isolate the wideband EMPs.

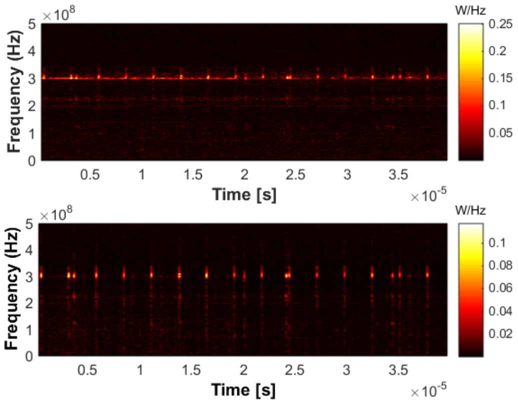

**Figure 2.** The top spectrogram displays the unfiltered experiment antenna measurement. In these data there are a number of continuous sources of RF interference that are obscuring a repeating wideband RF pulse. The bottom spectrogram displays the results of filtering the measurement. The continuous sources were able to be excised by leveraging their frequency content without nulling out or subtracting from the frequency content of the wideband pulses.

### 3.2 Time Dilation

A linear time dilation factor was developed to allow for the aggregation of multiple impact events to offset the different initial conditions in the impact plasma caused by differences in impactor parameters. The time of peak RF emission power in biased targets is a function of the initial plasma density. As the plasma undergoes thermal expansion, its Debye length increases and so does the penetration of any external electric fields into the impact plasma. A first order approximation used to determine when the bulk of the electrons in the impact plasma are accelerated by the external electric field is when the plasma Debye length is equal to the radius of the impact plasma.

A linear time dilation $T_i$, given by

$$T_i = \frac{\bar{\tau}}{\tau_i} \quad (2)$$

$$\tau_i = \left( \frac{Qe}{\frac{2}{3}\varepsilon_0 k_B T_e \pi} - r_{0,i} \right) \frac{1}{C_s} \quad (3)$$

was applied to a rolling ∼100 ns window power measurement for each impact. In Equation 2, $T_i$ is the linear time dilation factor applied to all times after the time of impact, for impact event $i$, $\bar{\tau}$ is the average time constant across all impact events for a set of experiments, and $\tau_i$ is the time constant for impact event $i$. In Equation 3, $k_B$ is the Boltzmann constant, $e$ is the magnitude of the charge on an electron, and $T_e$ is the electron temperature in kelvins, $Q$ is the amount of liberated charge, and $r_{0,i}$ is the impactor crator radius. The result of Equation 2 is that the time when the plasma's Debye length is equal to its radius is the same for all impact events regardless of different initial plasma densities.

## 3.3 Detection and Aggragation

An EMP is detected at time $t$ for impact event $i$ if the power at time $t$ is a predefined threshold $a$ above the average power for the entire observation of impact event $i$ as shown in Equation 4.

$$D_{t,i} = P_{t,i} \geq a\bar{P}_i \tag{4}$$

These results are then compiled by impact conditions to create EMP detection rate vs time plots for different impact conditions.

# 4 Results

EMP detection rates were computed for targets biased to 0V, -500V, and -1000V at the MPI facility, and for targets biased to 0V and -1000V at the CCLDAS facility. An increase in EMP detection rate was seen for targets with a strong negative bias within the first 500 ns after impact. The timing of these emissions correlates with the expected time the plasma's Debye length reaches the same order of magnitude as its spatial length. An EMP detection rate plot for -1000V targets at MPI is shown in Figure 3. A dependence on target bias was also observed, with more negatively biased targets producing more detectable EMPs.

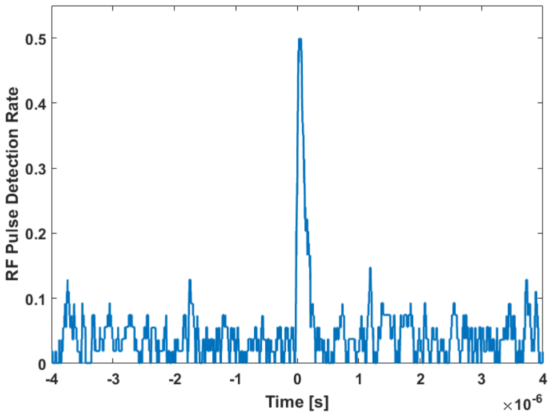

**Figure 3.** MPI summarized RF pulse detection rate for 54 measurements is displayed vs time as referenced to the time of impact on -1 kV biased targets. There is an approximate 10-fold increase in RF pulse detection 50 ns after impact.

Detections in the aggregated results aided the detection and isolation of EMPs on a case by case basis, which allows for a relationship to be formed between impactor mass and velocity and strength of EMP emissions. A power law relationship was developed between impactor mass and velocity and peak emitted electric field strength. This relationship is depicted in Figure 4. It was found that peak electric field strength scales approximately linearly with impactor mass and to the power of 3.5 with velocity.

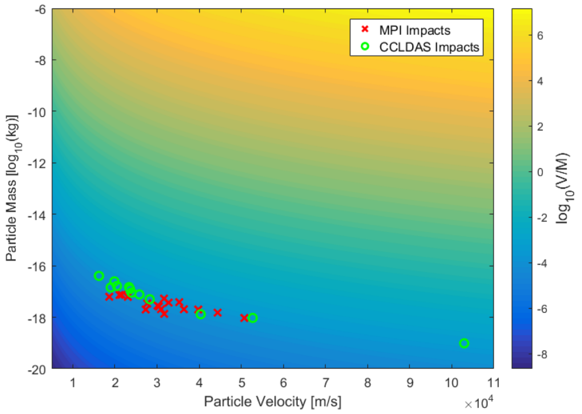

**Figure 4.** A peak electric field strength scaling law was derived for impacts on -1 kV biased targets using results from both MPI and CCLDAS. 30 impact events were utilized to derive this scaling. These electric field measurements and scaling law are taken at 10-20 cm from impact.

# 5 Conclusions

Experiments were conducted at multiple electrostatic accelerator facilities to investigate the potential for damaging EMP emissions from dust-sized hypervelocity impacts. Negatively biased targets were studied for their ability to produce EMPs from a bulk charge separation and acceleration of the impact plasma. Wideband RF pulses were detected at both MPI and CCLDAS facilities from impacts with negatively biased targets. The strongest emissions were observed in -1000 V biased targets, while weaker emissions were seen in -500 V biased targets. The RF emission are wideband, quickly decaying signals that appear 50-100 ns after impact in -1000 V impacts, and 200 ns after impact in -500 V impacts and decay within 100 ns.

A peak electric field scaling law was developed for the -1000 V impact cases. By extrapolating to micro and nanogram sized impacts, expected peak electric field strength from impact can reach kV/m orders of magnitude. This strength of electric field is well beyond many electronic component design specifications, placing satellites at risk from these type of emissions [5].

To truly understand the full risk spectrum, in situ measurements need to be taken as only a small subset of possible impactor masses and velocities can be re-created on the ground. In situ measurements also combine meteoroid flux with the evolution of charge states a spacecraft can experience to create a more complete picture of the threat.

# 6 Acknowledgments

This material is based upon work supported by the National Science Foundation Graduate Research Fellowship under Grant No. DGE-114747. The authors of this paper would also like to thank the teams at MPI, CCLDAS, and

Stanford, including Dr. Ivan Linscott, Ashish Goel, Monica Hew, Paul Tarantino, David Strauss, and Nicolas Lee for their contributions in collecting the hypervelocity impact data. The authors would also like to thank the Bosack-Kruger Foundation for sponsoring portions of the hypervelocity impact experiments in CCLDAS.

## References

[1] Kessler, Donald J., and Burton G. Cour-Palais. “Collision frequency of artificial satellites: the creation of a debris belt." Journal of Geophysical Research: Space Physics 83.A6 (1978): 2637-2646.

[2] Laurance, M. R., and D. E. Brownlee. “The flux of meteoroids and orbital space debris striking satellites in low Earth orbit." (1986): 136-138.

[3] Drapatz, S., and K. W. Michel. “Theory of shock-wave ionization upon high-velocity impact of micrometeorites." Zeitschrift fÃijr Naturforschung A 29.6 (1974): 870-879.

[4] A. Nuttall, M. Kochenderfer, and S. Close, “Detection of hypervelocity impact radio frequency pulses through prior constrained source separation," Radio Science, vol. 51, pp. 1-16, 2016

[5] Electromagnetic Environmental Effects Requirements for Systems, DoD Interface Standard Mil-Std 464C, 1 Dec 2010.

[6] Close, S., I. Linscott, N. Lee, T. Johnson, D. Strauss, A. Goel, D. Lauben, R. Srama, A. Mocker, and S. Bugiel, Detection of electromagnetic pulses produced by hypervelocity micro particle impact plasmas, Physics of Plasmas, vol. 20, 092102, 1-8, 2013, doi:10.1063/1.4819777.

[7] Lee, N., S. Close, D. Lauben, I. Linscott, A. Goel, T. Johnson, J. Yee, A. Fletcher, R. Srama, S. Bugiel, A. Mocker, P. Colestock, and S. Green, Measurements of freely-expanding plasma from hypervelocity impacts, Int. J. Impact Eng., 44, 40-49, 2012.

[8] Lee, N., S. Close, A. Goel, D. Lauben, I. Linscott, T. Johnson, D. Strauss, S. Bugiel, A. Mocker, and R. Srama, Theory and experiments characterizing hypervelocity impact plasmas on biased spacecraft materials, Physics of Plasmas, 20, 032901, 2013, doi:10.1063/1.4794331.